SLEEPJ, 2021, 1–12

doi: 10.1093/sleep/zsaa152
Advance Access Publication Date: 19 August 2020
Original Article

ORIGINAL ARTICLE

Largest scale dissociation of brain activity at propofol-induced loss of consciousness

Jesus Pujol[1,2,*], Laura Blanco-Hinojo[1,2], Lluís Gallart[3,4], Luís Moltó[3], Gerard Martínez-Vilavella[1], Esther Vilà[3], Susana Pacreu[3], Irina Adalid[3], Joan Deus[1,5], Víctor Pérez-Sola[2,6] and Juan Fernández-Candil[3]

[1]MRI Research Unit, Department of Radiology, Hospital del Mar, Barcelona, Spain, [2]Centro Investigación Biomédica en Red de Salud Mental, CIBERSAM G21, Barcelona, Spain, [3]Department of Anesthesiology, Hospital del Mar-IMIM, Barcelona, Spain, [4]Department of Surgery, Universitat Autònoma de Barcelona, Barcelona, Spain, [5]Department of Psychobiology and Methodology in Health Sciences, Autonomous University of Barcelona, Barcelona, Spain and [6]Institute of Neuropsychiatry and Addictions, Hospital del Mar-IMIM and Department of Psychiatry, Autonomous University of Barcelona, Barcelona, Spain

*Corresponding author. Jesus Pujol, MRI Department, Hospital del Mar, Passeig Marítim 25–29. 08003, Barcelona, Spain. Email: 21404jpn@comb.cat.

Abstract

The brain is a functional unit made up of multilevel connected elements showing a pattern of synchronized activity that varies in different states. The wake–sleep cycle is a major variation of brain functional condition that is ultimately regulated by subcortical arousal- and sleep-promoting cell groups. We analyzed the evolution of functional MRI (fMRI) signal in the whole cortex and in a deep region including most sleep- and wake-regulating subcortical nuclei at loss of consciousness induced by the hypnotic agent propofol. Optimal data were obtained in 21 of the 30 healthy participants examined. A dynamic analysis of fMRI time courses on a time-scale of seconds was conducted to characterize consciousness transition, and functional connectivity maps were generated to detail the anatomy of structures showing different dynamics. Inside the magnet, loss of consciousness was marked by the participants ceasing to move their hands. We observed activity synchronization after loss of consciousness within both the cerebral cortex and subcortical structures. However, the evolution of fMRI signal was dissociated, showing a transient reduction of global cortico-subcortical coupling that was restored during the unconscious state. An exception to cortico-subcortical decoupling was a brain network related to self-awareness (i.e. the default mode network) that remained connected to subcortical brain structures. Propofol-induced unconsciousness is thus characterized by an initial, transitory dissociated synchronization at the largest scale of brain activity. Such cortico-subcortical decoupling and subsequent recoupling may allow the brain to detach from waking activity and reorganize into a functionally distinct state.

Statement of Significance

The neural basis of consciousness is one of the greatest challenges to the scientific worldview. Neuroimaging research increasingly contributes to characterizing the states of consciousness providing accurate pictures of their functional anatomy. Most studies identify differences between wakefulness and established unconsciousness. However, less is known of the functional events mediating the moment we fall asleep. We directly assessed the transition to unconsciousness induced by a hypnotic agent using a dynamic characterization in the difficult MRI environment. We observed that induced unconsciousness is characterized by a transient dissociated synchronization at the largest scale of brain activity. We propose that such cortico-subcortical decoupling and subsequent recoupling may allow the brain to detach from waking activity and reorganize into the functionally distinct state.

Key words: neuronal synchrony; functional state transitions; brainstem; functional connectivity; sedation; cerebral cortex

Submitted: 15 May, 2020; **Revised:** 6 August, 2020

Introduction

The brain is a high energy system composed of multilevel connected elements. The overall activity pattern of inter-neuronal communications provides the individual with a functional entity that varies in the form of different states. The wake–sleep cycle is a major variation of brain functional condition, reflecting a balance change in the capacity to integrate information from environmental sources and internal drivers [1–3].

The wake–sleep transition ultimately depends on the arousing effect of deep brain structures on the whole cerebral cortex. The ascending arousal system in the upper brainstem (and diencephalon) is central for maintaining the cortex in an activated state, whereas elements of the hypothalamus may act as a switch for transitioning into slumber by shutting down the ascending arousal system [1, 4]. The sleep-regulating subcortical structures, however, do not only control brain arousal, but also contribute to modulating many aspects of activity in each brain state. Indeed, the ascending arousing system includes cell groups of the major neuromodulatory systems such as the dorsal raphe (releasing serotonin), tubero-mammillary nucleus (histamine), ventral tegmental area (dopamine), laterodorsal and pedunculopontine tegmentum (acetylcholine), perifornical lateral hypothalamus (orexin), ventral periaqueductal gray (dopamine), and locus coeruleus (norepinephrine) [1, 4].

The transition into natural or drug-induced sleep involves strong cortical changes typically characterized by an increase in low-frequency EEG activity indicating widespread cortical synchronization expressing neural function inhibition, which follows a firing reduction in arousal-promoting neurons [1]. Interestingly, the complete transition to the new cortico-subcortical functional equilibrium in the sleep state is not instantaneous and generally takes place over a few seconds in rodents or a few minutes in humans [1], which is in contrast to the apparent abruptness of falling asleep.

Neuroimaging research increasingly contributes to characterizing the states of consciousness in a different temporal scale and providing accurate pictures of the functional anatomy. Propofol is a hypnotic agent that increases GABA-mediated inhibition [5], which can be used to induce loss of consciousness in a controlled manner [6–8]. Most studies have been developed to identify substantial differences in functional MRI (fMRI) measures between wakefulness and established unconsciousness induced by propofol (e.g. [9–21]) and, to a lesser degree, to ascertain the functional events mediating the moment we lose consciousness. A number of fMRI studies on natural sleep, however, suggest that the initial light-sleep stage is actually a transition between wakefulness and sleep involving a temporary cortical synchronization [22–25] and alteration of cortical–subcortical relationships [23, 24]. In this way, a recent study to explore the complex repertory of large-scale brain dynamics characterizing each natural stage of slumber further supports the view that light sleep (stage N1) is a transitional functional state qualitatively distinct from both wakefulness and sleep [26]. Transient functional connectivity changes may also be present during the return of consciousness after sedation [27].

In terms of functional connectivity MRI, there is a degree of synchrony among all major brain elements beyond specific network activity coupling and decoupling [28–32]. At the largest scale, synchronization of brain activity depends on the reciprocal interactions between the cerebral cortex and the modulatory subcortical cell groups [32–35]. However, cortico-subcortical functional relationships need to be adjusted in each behavioral state [2, 35, 36]. In such a context, we posited that the coupling between the cortex and deep brain structures regulating wake–sleep transitions would be transitorily dissociated during the induced loss of consciousness until the brain reorganized into the new state. That is, the interruption of current reciprocal cortico-subcortical influences may arguably facilitate the balance change in terms of the capacity to integrate information from environmental sources and internal drivers [1–3]. To investigate this proposal, we used a dynamic approach and analyzed the evolution of fMRI signal in the whole cortex and in a deep region including most sleep-regulating subcortical nuclei at loss of consciousness induced by the hypnotic agent propofol.

Methods

Study participants

A total of 30 healthy right-handed participants, including 18 males and 12 females (mean: 26.9 years; *SD*: 5.3 years) made up the initial study sample. Participants were recruited from the University environment through advertisements and were required to meet the criterion of the American Society of Anesthesiologists (ASA) physical status ASA I (healthy, nonsmoking, no or minimal alcohol) [37] to be eligible. A complete medical interview, physical exam, ECG, and blood point-of-care testing (blood gases, electrolytes, glucose, and hemoglobin) were carried out to exclude subjects with medical or neurological disorders, psychiatric illness, substance abuse, body mass index < 18 or > 30 kg/m^2, pregnancy, known allergy to anesthetics, and claustrophobia. None of the subjects was undergoing medical treatment.

This study was conducted in accordance with the principles expressed in the Declaration of Helsinki. The protocol was approved by the Ethical Committee of Clinical Research of the Parc de Salut Mar of Barcelona (reference no 2017–7165) and by the Spanish Agency of Medicines and Medical Devices, AEMPS (reference 5NFNF6V55C). Written informed consent was obtained from all participants. Participants were paid for their contribution.

Experimental procedure

With the aim of inducing unconsciousness using propofol, a procedural sedation regimen was used as in diagnostic ambulatory procedures, but at a slower infusion rate (see later section). Sedation procedures were adapted to the constraints of the MRI environment: (1) the dose of propofol was thus individually adjusted to induce the desired level of unconsciousness within the fMRI acquisition time window, (2) "loss of conscious control" was objectified during fMRI, and (3) the sedation level was clinically verified after the acquisition, while maintaining the steady-state doses of propofol reached during fMRI. At the attained level, the individual no longer responds to verbal prompting, but can be awakened with relatively intense stimulation, although breathing is spontaneous with no need for tracheal intubation.

A behavioral estimation of "loss of conscious control" was used as a surrogate of conventional "loss of consciousness," which cannot be fully assessed during MRI acquisition (i.e.

using awaken stimulation) without interfering in the neural processes to be investigated. Participants were instructed to repeatedly squeeze a soft pneumatic balloon with their right hand at a rate of approximately one movement every 3 s throughout the MRI with their eyes open while they were awake. The time course for squeezing was monitored on-line running a data logger developed in-house with Labview 8.0 software (National Instruments Corp., Austin, TX). Loss of conscious control was marked by the participants ceasing to move their hands. Although this behavioral reference is not equivalent to loss of consciousness, it was however useful to direct our fMRI analysis. Transition into induced unconsciousness should necessarily occur after losing conscious motor control. However, loss of conscious control may or may not coincide with full awareness interruption.

Anesthetic technique

During the experiment, fMRI was continuously acquired for a total of 15 min. In the initial 3-min baseline period, no drug was administered. Subsequently, a continuous intravenous infusion of propofol commenced using a target-controlled infusion system (Base Primea Orchestra®, Fresenius Kabi, Brézins, France), individually programmed at a target plasma concentration of 3.5 mcg/mL based on the Schnider model [38]. Propofol target plasma concentration was steeply increased by 0.5 mcg/mL every 2 min until the participant ceased to move his or her hand for at least 20 s (note that the response to verbal command was not assessed during image acquisition). At this moment (20 s after loss of conscious control), propofol target-controlled infusion was targeted at the effect-site (brain) concentration currently estimated by the model.

Physiological monitoring

Monitored physiological parameters included electrocardiography (ECG), pulse oximetry (SpO2), expired CO_2 measured by oral and nasal capnography cannulas (Oral-Trac®, Salter Labs, Arvin CA), and respiration oscillations registered using a thoracic pneumatic belt (Philips 3T Breathing Belt) and displayed real-time using Labview software (National instruments Corp., Austin, TX). Oxygen (2 L/min) was administered throughout the study. Participants were fasted 8 h for solids and 2 h for water.

MRI acquisition

A Philips Achieva 3.0 Tesla magnet (Philips Healthcare, Best, The Netherlands), equipped with an eight-channel phased-array head coil and single-shot echoplanar imaging (EPI) software, was used for the MRI assessment. The functional blood oxygen level-dependent (BOLD) sequence consisted of gradient recalled acquisition in the steady state (time of repetition [TR], 2,000 ms; time of echo [TE], 35 ms; pulse angle, 70°) within a field of view of 240 × 240 × 128 mm, with a 64 × 64-pixel matrix, and a slice thickness of 4 mm (inter-slice gap, 0 mm) and acquisition voxel size of 3.75 × 3.75 × 4 mm. A total of 34 interleaved slices were acquired to cover the whole-brain. Each functional time series consisted of 450 consecutive image sets or volumes obtained over 15 min. The first four (additional) image sets in each run were discarded to allow the magnetization to reach equilibrium.

MRI preprocessing

Imaging data were processed using MATLAB version 2016a (The MathWorks Inc, Natick, MA) and Statistical Parametric Mapping software (SPM12; The Wellcome Department of Imaging Neuroscience, London). Preprocessing involved motion correction, spatial normalization, and smoothing by means of a Gaussian filter (full-width half-maximum, 8 mm). Data were normalized to the standard SPM-EPI template and resliced to 2 mm isotropic resolution in Montreal Neurological Institute (MNI) space. All image sequences were inspected for potential acquisition and normalization artifacts. At this stage, 9 participants were removed from the initial sample of 30 subjects as a result of large head displacements preventing adequate image preprocessing (3 cases) and motion artifacts affecting image volumes obtained just after the behavioral reference of loss of conscious control (6 cases). Specifically, a period of at least 90 s (45 volumes) with no motion artifacts was required participants to be included in further analyses.

MRI analyses

We analyzed the evolution of fMRI BOLD signal in the whole cortex and in a deep region including most sleep-regulating subcortical nuclei at the transition into unconsciousness induced by propofol. The analysis included: (1) fMRI BOLD signal extraction, (2) individual analysis by plotting signal time courses in both study regions for each participant, and (3) group analyses using a common reference point, which served to anchor signal oscillations and average out signal time courses across participants.

BOLD signal extraction

fMRI signal was extracted using MarsBaR region-of-interest (ROI) toolbox in MNI stereotaxic space in 21 participants. The study primary analysis included data from the whole cortex and a single subcortical region. The fMRI signal was extracted separately for each hemisphere by calculating the mean ROI value at each point across the time-series within an anatomically defined gray matter mask of the entire hemisphere (SPM gray matter mask at a gray matter probability of 40%). One single cortical measure was finally obtained by averaging the data from both hemispheres (total 1,227.8 mL). As for the subcortical region, the fMRI signal was extracted from a tissue volume defined by a 17 mm radial sphere centered at the midbrain tegmentum (MNI x, y, z; 0, −20, −10 mm, total 20.4 mL). This region includes most sleep-regulating subcortical nuclei [4] (Supplementary Figure S1). The extracted fMRI signal time series were then mean-centered (demeaned) and a high-pass filter set at 128 s was applied using the REST toolbox [39].

In addition to the primary whole cortico-subcortical analysis, the evolution of the fMRI BOLD signal was also assessed in selected regions corresponding to functionally relevant brain systems. MarsBaR ROI toolbox was similarly used to extract fMRI signal in eight cortical, 5 mm-radius ROIs. These regions included the somatosensory cortex (MNI; −44, −32, 54), visual cortex (MNI; 4, −88, −8) and supplementary motor area (MNI; −4, −2, 50) identified in healthy volunteers using a multisensory task [40]. The posterior cingulate cortex (MNI; −3, −54, 30) was included as a main element of the default mode network [41], the dorsal frontal cortex (MNI; 28, −10, 58) as part of the dorsal

attention network [42] and a series of anatomically identified regions such as the posterior inferior frontal sulcus (MNI; 44, 12, 28), as part of the ventral attention system, the posterior inferior frontal gyrus (pars triangularis-Brodman area 45; MNI; 44, 26, 4) and the posterior superior temporal sulcus (MNI; 52, –36, 2).

Within the main subcortical region, additional BOLD signal extractions were performed for a 5 mm-radius ROI centered at the midbrain tegmentum (MNI; 0, –20, –10 mm) and a 5 mm-radius (bilateral and averaged) ROI centered at the hypothalamus (MNI; ±4, –8, –8) to separately illustrate the dynamics of the brainstem and diencephalon, respectively (Supplementary Figure S1) [4].

Individual BOLD signal analysis

The fMRI time series from the cortex and subcortical region were plotted in each individual to identify common features across participants. The most consistent feature involved a global signal decrease followed by a global signal increase at a variable delay from the moment the participants stopped moving their hand. The point at which the fMRI signal crossed the zero value in the mean-centered cerebral cortex time series (see the Results/Figures section) was individually identified and served as the reference fMRI volume for subsequent group analyses.

Group analysis

To analyze the transition to unconsciousness, a total of 60 fMRI volumes (2 min) were used from each valid case (n = 15, see the Results section) that included the reference volume, the 11 preceding volumes and the 48 succeeding volumes. SPM maps were obtained using group-average BOLD signal time courses from the cerebral cortex and the subcortical region as regressors in first-level analyses that also included six motion estimates as co-variables and removal of volumes with inter-frame motion >0.3 mm [43]. Resulting first-level contrast images were carried forward to second-level analyses in SPM. One-sample t-test maps were estimated for both cortical and subcortical models. A motion summary measure (mean inter-frame motion [44]) for each participant was included as a covariate to further control potential motion effects. Results were considered significant when clusters formed at a threshold of $p < 0.005$ survived whole-brain family-wise error (FWE) correction ($p < 0.05$), calculated using SPM.

Volume-by-volume fMRI mapping

Volume-by-volume (TR, 2 s) maps were generated with group-average images from the transition period analyzed in 15 participants. Specifically, non-thresholded one-sample t-tests were used to generate such mean group images. Finally, the obtained 60 images (frames) served to generate a movie sequence of the cortical and subcortical fMRI signal evolution on a mid-sagittal anatomic slice. Movie frame transitions were smoothed using a sliding window (3 images averaged) and 10-step morphing sequencing (using Fantamorph software, v. 5.0, Abrosoft, Devon, UK).

Finally, to statistically test fMRI BOLD signal changes at the transition into unconsciousness, the fMRI signal was also extracted in 2-min periods of baseline (no propofol), sedation (propofol-sedated but awake), transition period, and after the transition period (with enough data from this last period in 13 participants only). The paired t-test was used to statistically test differences in the standard deviation (*SD*) of fMRI signal between baseline and the transition period. Standard deviation change (taken as a surrogate measure of the amplitude of an oscillating signal) was used as an estimation of neural synchrony change. The *SD* of a sine oscillating signal directly expresses the amplitude of the oscillation in accordance with the equation "amplitude = $2\sqrt{2}$ *SD*" [45]. And, in large-scale oscillations, amplitude changes are considered to result from changes in phase synchronization within a neural ensemble [46], particularly during states of neural inhibition such as sleep or sedation [2, 35, 47–49]. Standard deviation is preferable to the use of amplitude if the acquired signals do not show a well-defined peak-to-peak value [45].

Interactions between time period (baseline vs. transition) and fMRI signal coupling (cortico-cortical vs. cortico-subcortical Pearson correlation) were tested using repeated measures ANOVA. This analysis was also performed using fMRI signals previously adjusted to global brain signals.

Results

Estimated propofol target plasma concentration [38] 20 s after the participant ceased to move his or her hand in the study group showed a mean of 4.4 mcg/mL (*SD*, 0.8 mcg/mL) and the measured effect site concentration 3.8 mcg/mL (*SD*, 0.6 mcg/mL).

Participants squeezed the soft pneumatic balloon with an actual mean rate of 0.30 Hz (*SD*, 0.08 Hz) throughout the MRI prior to loss of conscious control. Hand-movement cessation was characterized by a gradual reduction in both amplitude and frequency. In the last minute prior to discontinued movement, the amplitude was reduced by a mean of 46% (*SD*, 46%) and movement frequency was 0.19 Hz (*SD*, 0.09 Hz).

We firstly analyzed the temporal evolution of the fMRI signal for both the cerebral cortex globally and the subcortical region containing most sleep-regulating cell groups on an individual basis. A notably common phenomenon was observed after our behavioral reference of loss of conscious control (stopping moving the hand). Figure 1 shows individual cases that best illustrate the key study result. The phenomenon was characterized by a dissociated phase synchronization of the fMRI signal. The amplitude of fMRI signal oscillations increased (together with a reduction of the dominant frequency) in both the cortex and the subcortical region, indicating activity synchronization at both levels. However, the signal synchronization phenomenon evolved with a different timing, with the cortical changes progressing earlier and showing an initial signal fall (Figure 1).

Some evidence of decoupled signal oscillation was observed in 19 of the 21 participants analyzed. The initial signal fall began just after the participants stopped moving their hand in nine participants (specifically after a mean of 2.9 s and *SD* of 3.9 s). In the remaining group of 10 participants, the initial signal fall variably began after a temporal lapse (mean, 61.0 s; *SD*, 25.1 s). In no case was the cortico-subcortical dissociated synchronization of fMRI signal evident before the participants ceased to move their hand.

The described dynamics were notably reproducible across subjects. Thus, the data allowed us to perform a group analysis by averaging fMRI time courses from 15 of the 19 participants with evidence of dissociated synchronization (the signal

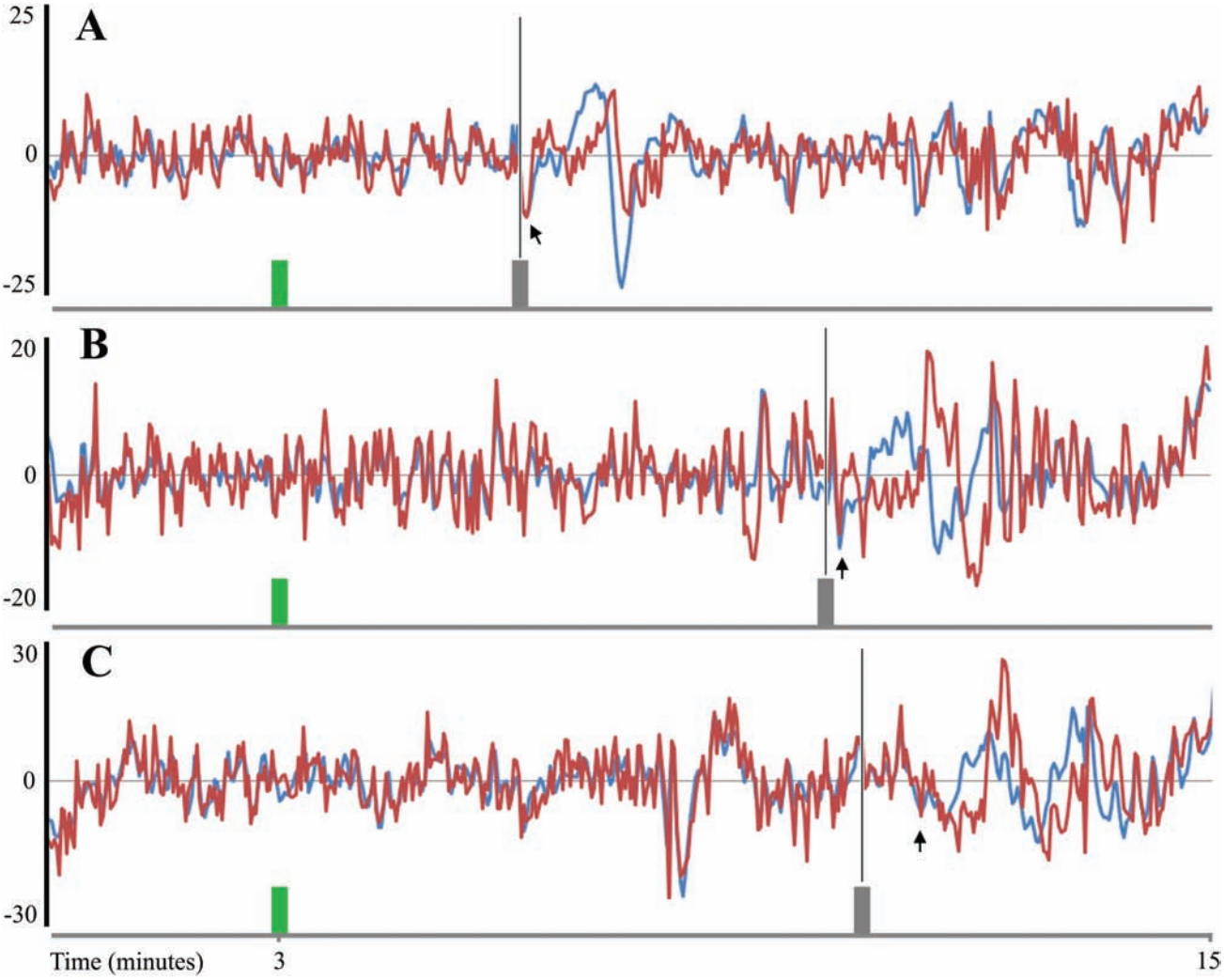

Figure 1. Individual cases illustrating the dissociated synchronization of fMRI signal evolution (arbitrary units) in the cerebral cortex (blue line) and subcortical structures (red line). Green vertical bars indicate the moment the continuous intravenous infusion of propofol began. Gray vertical bars indicate loss of conscious control. In participant A, loss of conscious control was an early event and the initial signal fall (arrow) coincided with the moment of loss of conscious control. In participant B, loss of conscious control was a late event. In participant C, a lapse of 40 s occurred between the loss of conscious control and the initial signal fall (arrow).

oscillation was not complete in 2 cases occurring at the end of fMRI acquisition and 2 cases showing late head-motion artifacts). The across-subject averaged time course of the entire cortex in the selected transition period confirmed the occurrence of a very slow fMRI signal oscillation involving an initial signal fall followed by a rise-and-fall cycle with a total duration of 1 min and 40 s (Figure 2, bottom).

Figure 2 (top) shows conventional SPM maps of brain areas with significant correlation with the group-average cortical time course. The brain systems showing the closest fitting included the visual, auditory, and somatosensory cortices, the cortical motor system, the dorsal fronto-parietal attentional system and language areas (Figure 2 and Supplementary Table S1). However, a brain display at a lower threshold indicated that cortical synchronization was highly global. Interestingly, the frontal pole and part of the angular gyrus showed the weakest correlation with group-average time course.

Figure 3 shows group-average time courses for the whole subcortical region, midbrain tegmentum and the posterior hypothalamus. As in the illustrative single-subject cases, a delay was evident in the evolution of subcortical region synchronization with regard to cortical synchronization. The highest fMRI signal decoupling occurred with the hypothalamus during almost the entire period. Relevantly, the hypothalamic signal remained at a relatively higher level during the initial cortical signal fall.

Figure 3 and Supplementary Table S1 show regions with significant correlation with the subcortical time courses. The maps include the midbrain-diencephalon junction, midbrain tegmentum, hypothalamus, nucleus accumbens, cerebellar vermis, amygdala, and hippocampus. In addition, we found two cortical regions significantly coupled with the subcortical fMRI signal time courses, namely the left angular gyrus (a component of the default mode network) and the prefrontal cortex at the frontal pole.

The dissociation of the global synchronization was further illustrated by a dynamic display showing volume-by-volume (temporal resolution of 2 s) group images of the transition period analyzed. Figure 4 shows a mid-sagittal slice at representative time points (selected frames) and the whole movie display is provided as Supplementary Material Video.

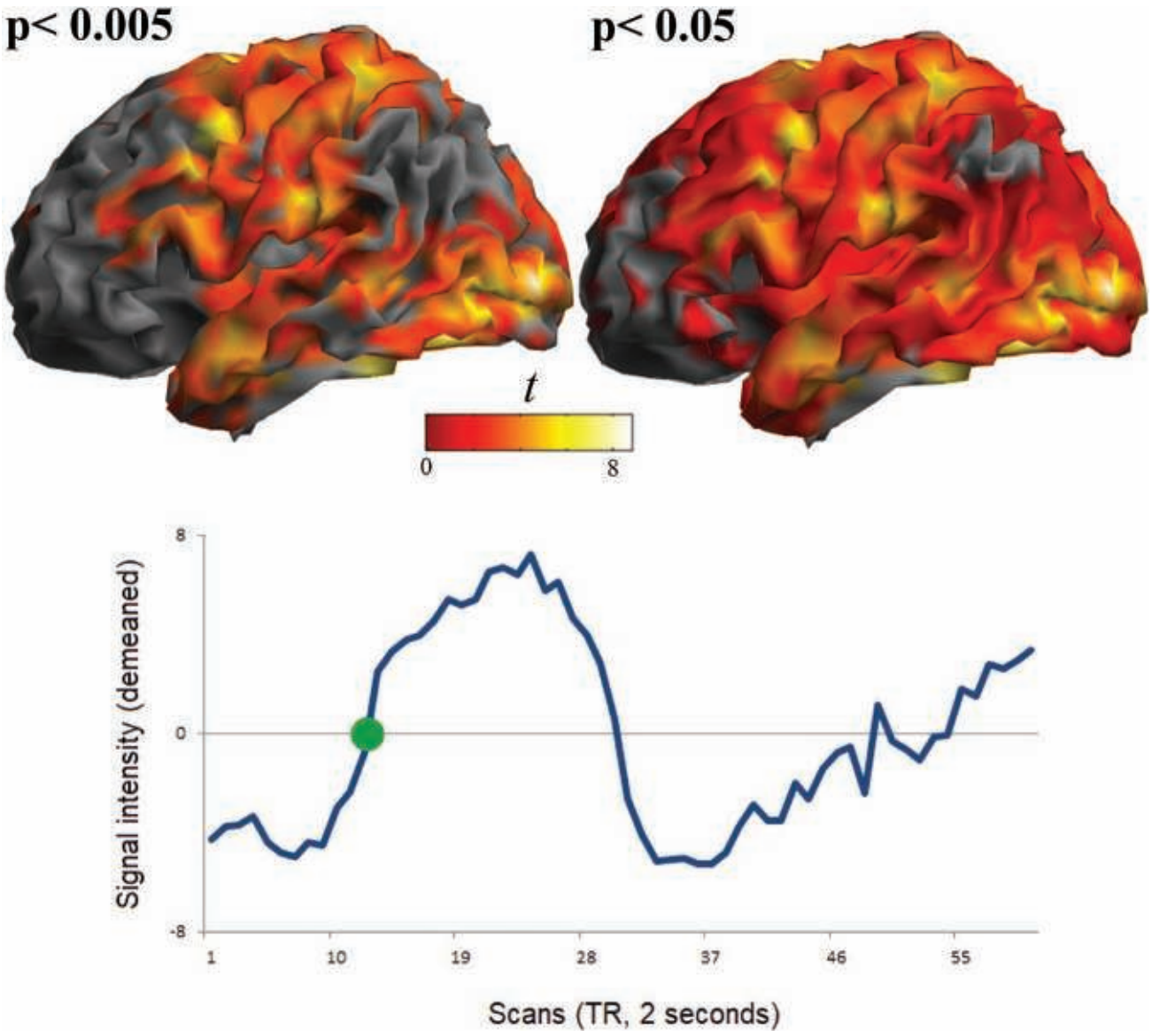

Figure 2. Group-level cerebral cortex analysis. The plot (bottom) corresponds to the cerebral cortex fMRI BOLD signal time course of the selected 2-min transition period averaged across 15 participants. SPM maps (top) correspond to the correlation between the averaged time course and the fMRI BOLD signal in the cerebral cortex, voxel-wise (thresholded at $p < 0.005$ and $p < 0.05$). The green spot indicates the common reference volume individually identified in order to average signal oscillations across participants. Transition to unconsciousness was considered to occur previously, at the initial signal fall.

Quantitative analyses were performed to statistically test both brain synchronization and cortico-subcortical dissociation. The *SD* of the fMRI signal oscillation was used as a measure of region synchrony. We found a highly significant *SD* change from baseline to the transition period in both the cortex (paired $t_{(14)} = 5.8$; $p = 0.00005$) and the subcortical region (paired $t_{(14)} = 5.5$; $p = 0.00008$). *SD* differences between baseline and unconsciousness were not significant (cortex paired $t_{(12)} = 1.8$; $p = 0.088$ and subcortical region (paired $t_{(12)} = 1.3$; $p = 0.195$), thus indicating that the synchronization phenomenon was robust only during the transition period. Data plots are presented in Figure 5 illustrating the parallelism of fMRI signal synchrony evolution in the cortex and the subcortical region in four 2-min periods (i.e. baseline, sedation, transition, and unconsciousness).

Synchronization during the transition period was therefore a robust phenomenon in both the cortex and subcortical structures. However, this within-region synchronization concurred with statistically significant cortico-subcortical decoupling. Figure 6 plots illustrative data showing to what extent the correlation of fMRI signal between cortical areas increases from baseline to the transition period, while the correlation between each cortical area and the subcortical region decreases. The interaction between time period (baseline vs. transition) and fMRI signal coupling (cortico-cortical vs. cortico-subcortical correlation) was significant for each brain system. Figure 6 also illustrates that the cortico-subcortical dissociation was generally reversed after the transition period (in no case were interactions significant when comparing data from baseline and unconsciousness periods). Although a limited number of brain systems were chosen from those most relevant to loss of consciousness with the aim of illustrating the phenomenon in Figure 6, we should emphasize that cortico-subcortical dissociation was largely a general event.

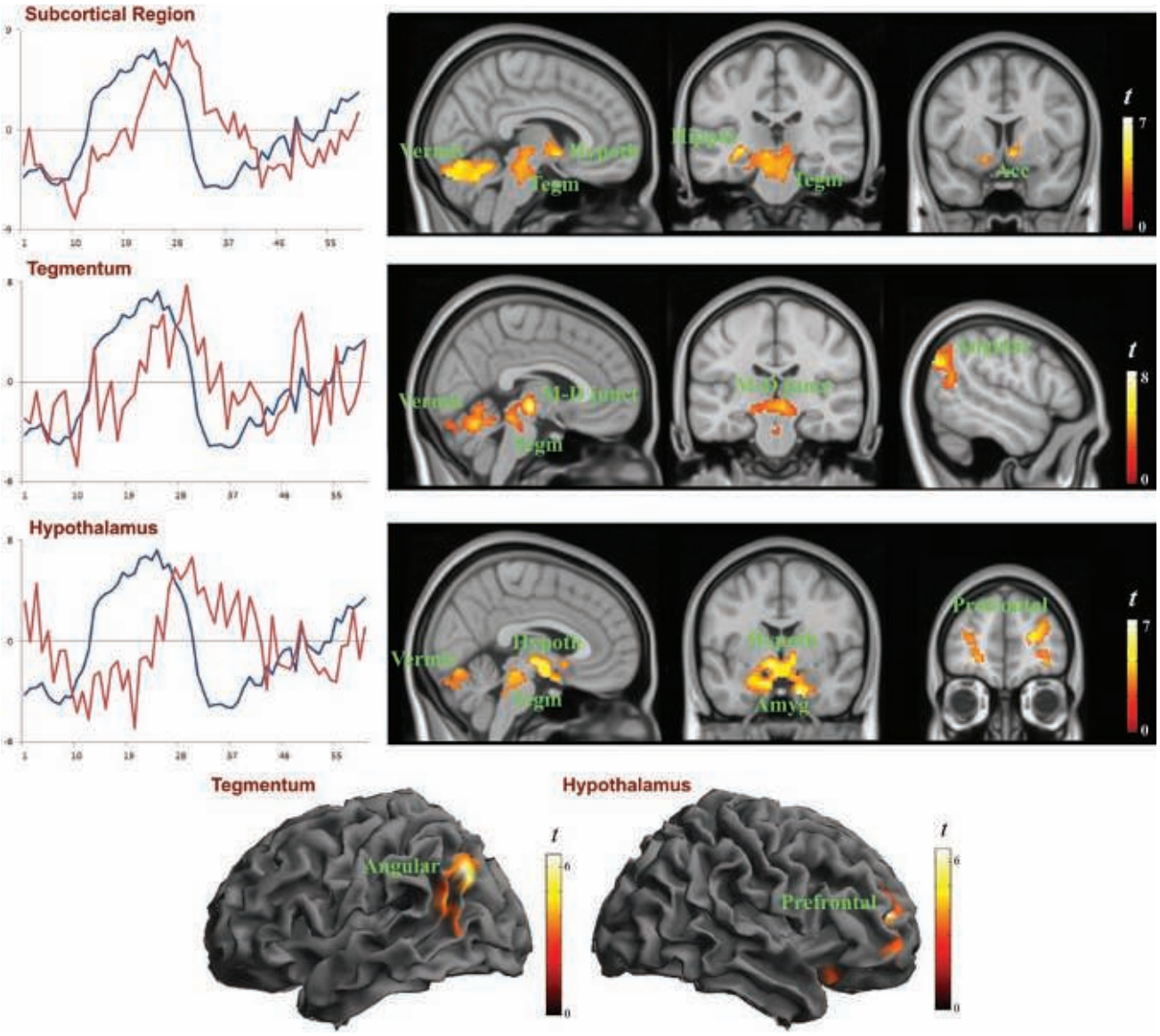

Figure 3. Group-level subcortical region analysis. The red lines in the plots (left) correspond to group-average fMRI signal time course of the selected 2-min transition period for the whole subcortical region, the midbrain tegmentum, and the posterior hypothalamus, overlaid on the cerebral cortex time course (blue lines). SPM maps (right and bottom) show regions with significant correlation with the corresponding subcortical time courses. Hypoth, hypothalamus; Hippoc, hippocampus; Tegm, tegmentum; Acc, nucleus accumbens; M-D junct, midbrain-diencephalic junction; Amyg, amygdala.

It is relevant to mention that the strength of correlation between default mode network regions and regions of typically anticorrelated systems (e.g. supplementary motor area, SMA) increase from baseline to transition, indicating that cortical synchronization takes place at the highest order of cortical organization. In this case, the interaction between time period and fMRI coupling was also highly significant. However, the coupling between the posterior cingulate cortex and the subcortical region did not decrease from baseline to the transition period (Figure 6). This effect further indicates that a few cortical elements are not detached from subcortical systems at transition including the posterior cingulate cortex, and also the left angular gyrus (another component of the default mode network) and the prefrontal cortex at the frontal pole (Figure 3).

Although the dissociation of brain synchronization was observed as a robust phenomenon affecting raw fMRI signal, the analysis was repeated after adjusting the data for global brain signal. We found that cortico-subcortical dissociation substantially remained after the adjustment (Supplementary Figure S2). All in all, the results would indicate that cortico-subcortical dissociated synchronization is both a global and a system-specific phenomenon.

Discussion

The temporal evolution of fMRI signal during the transition to propofol-induced unconsciousness is characterized by a dissociation of neural coupling at the brain's largest scale. After an initial signal fall, enhanced synchrony was observed in both the cerebral cortex and subcortical structures. However, this phenomenon evolved in a dissociated manner, with the cortical changes progressing earlier. Cortico-subcortical coupling

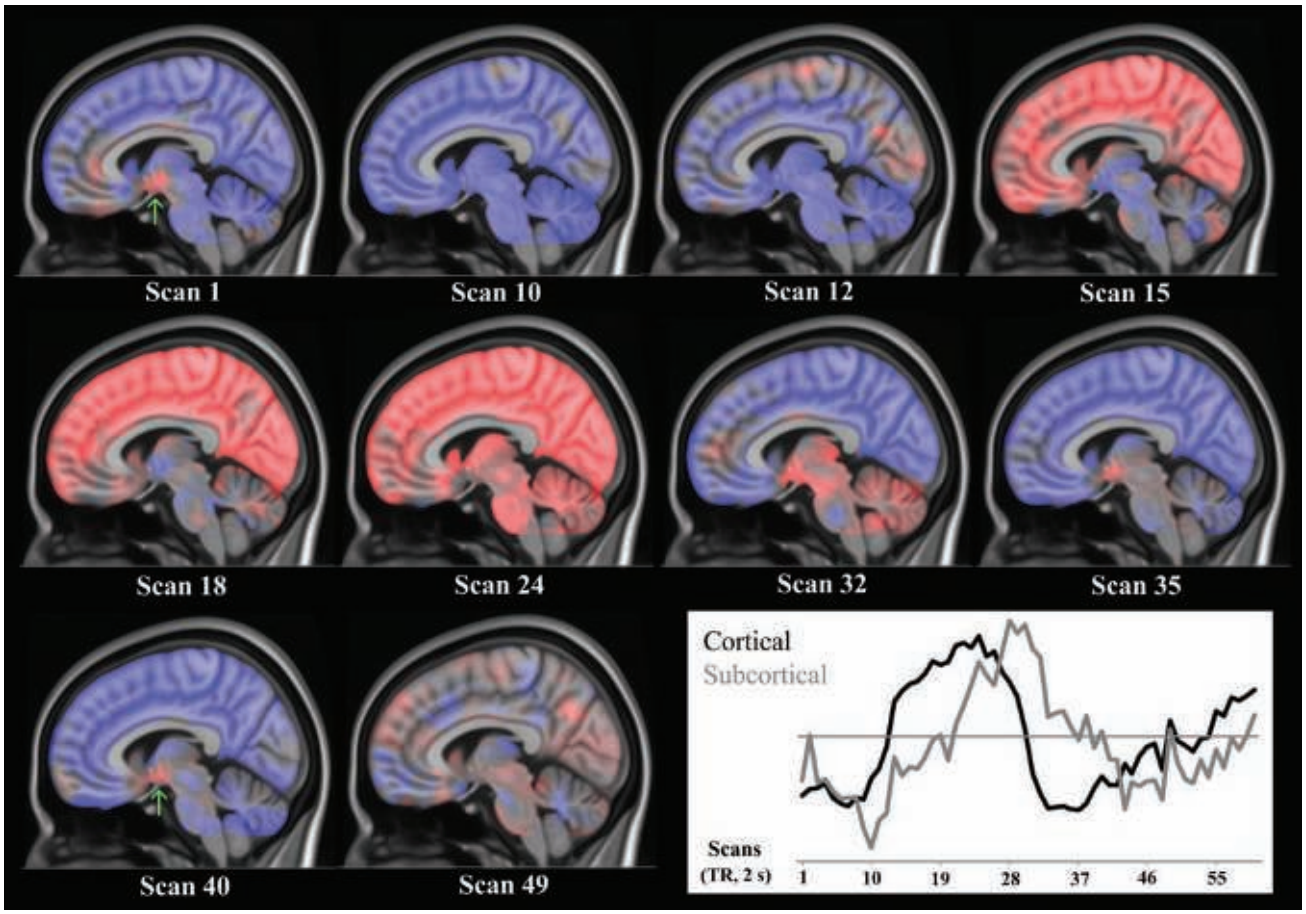

Figure 4. Representative volume-by-volume group images of the transition period. Blue indicates a low relative fMRI signal level (below signal time course mean) for the whole brain, whereas red indicates the opposite condition (signal above the series mean). The plot shows the evolution of fMRI signal separately for the cortical and subcortical regions-of-interest. The image sequence accurately illustrates the cortico-subcortical dissociation of fMRI signal evolution, which is most obvious in scans 15 and 32. Note also the hypothalamus (arrow) showing relatively higher fMRI signal in early (scan 1) and late (scans 35 and 40) dissociation moments.

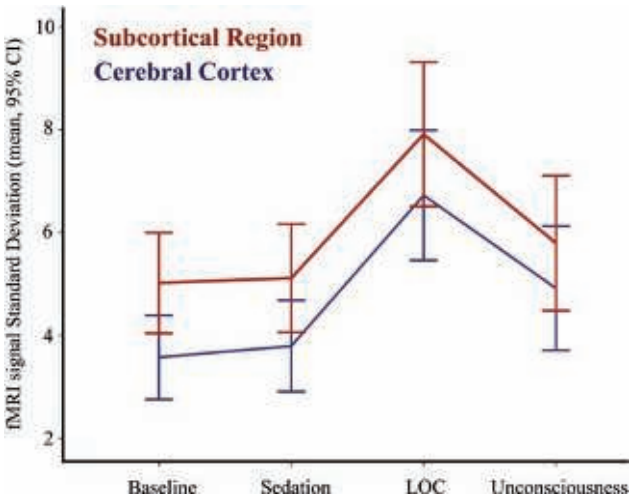

Figure 5. The parallelism of fMRI signal evolution in the cortex and the subcortical region in terms of region synchrony. The SD of functional MRI signal oscillations for a given period was used as measure of region synchrony. LOC denotes loss of consciousness and CI confidence interval.

was then restored after a complete, slow fMRI signal oscillation. Relevantly, distinct signal evolutions were observed for the brainstem and hypothalamus.

Behaviorally, loss of consciousness is a relatively abrupt event in both natural sleep and sleep induced by sedative agents. In our study, the described fMRI changes started in the form of signal fall implicating most of the gray matter, which may arguably be a physiological correlate of becoming unconscious. However, the whole fMRI signal transition phenomenon lasted approximately 100 s. This may be a slow process, in the range of the slowest fMRI signal oscillations reported in functional connectivity studies [46, 50], but it is consistent with the duration of EEG widespread cortical synchronization indicating full transition into sleep in humans [1, 51]. EEG data and the current fMRI results thus suggest that the transition into natural sleep or drug-induced unconsciousness is not complete upon the initial loss of consciousness.

Although cortical synchronization was global, the strength of correlation with the mean cortical signal time course varied across different cortical areas. High correlation was observed in a broad extension of the visual, auditory, and somatosensory cortices, the most dorsal aspect of the frontal and parietal lobes, and fronto-temporal cortex including Broca's and Wernicke's areas (Figure 2). This set of neural systems mostly expressing mean cortical synchronization interestingly corresponds to systems responsible for relevant components of wakefulness, such as sensory input awareness, and voluntary control of attention and inner speech [6, 52, 53].

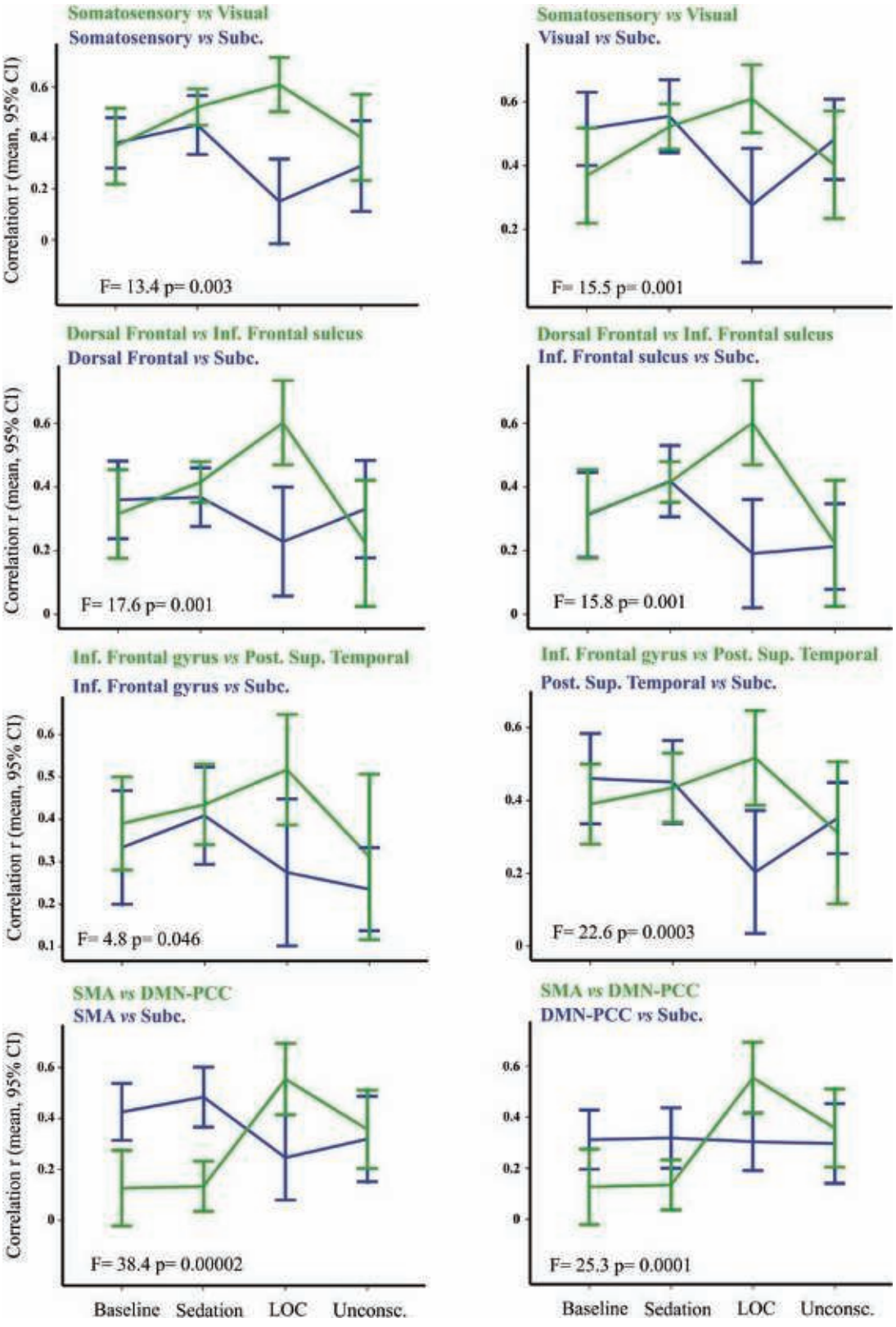

Figure 6. Functional MRI signal correlation between regions in different periods. The plots show group data (mean and 95% CI) from individual estimations of the correlations (Pearson *r*) of fMRI signal between two cortical regions (green), and a cortical region with the subcortical region (blue). The correlation of fMRI signal between cortical areas increased from baseline to the transition period, whereas the correlation between each cortical area and the subcortical region decreased. The statistics *F* and *p* correspond to the interaction between time period (specifically baseline vs. transition) and fMRI signal coupling (cortico-cortical vs. cortico-subcortical correlation). LOC, loss of consciousness. Unconsc., unconsciousness.

Our results also indicate that part of the cerebral cortex partially escapes from both global cortical coupling and cortico-subcortical decoupling. Indeed, the frontal pole and the angular gyrus showed low correlation with the mean cortical signal time course (Figure 2) and significant correlation with subcortical time courses (Figure 3). Also, the posterior cingulate cortex remained functionally connected to the subcortical systems at transition (Figure 6). The angular gyrus and the posterior cingulate cortex are major elements of the default mode network, which is relevant for both self-awareness and the conscious access to autobiographical storage in the wake state [54–57]. Although some previous fMRI studies have reported reductions in functional connectivity in the default mode network as part of a general breakdown induced by propofol in the cerebral functional architecture (e.g. [9, 20, 58]), partial network preservation and reorganization was also common in such studies [9, 19, 58–61] and, relevantly, in natural sleep (e.g. [23, 24, 26, 62]). Our results may further suggest that the default mode network (and the frontal pole) may play a role in generating a level of consciousness in the sleep state.

Indeed, sleep is only a "relative" state of loss of consciousness. Sensory input awareness and the voluntary control of behavior are certainly lost, but individuals may have vivid and fully conscious experiences during sleep modulated by internal drivers that are not, however, encoded for long-term storage and posterior recall [52, 63]. This is valid for both slow-wave and REM natural sleep [64], but also for propofol-induced unconsciousness, characterized by the frequent experience of dreams [52, 65]. The default mode network might thus also contribute to generating the sense of self during sleep and allowing us to be the agent of dreams and vivid experiences.

Regions showing significant correlation with subcortical fMRI signal time courses included key elements of the sleep-regulating system [1] located at the brainstem tegmentum, the diencephalon-midbrain junction, and the hypothalamus, but also in other apparently less critical structures such as the cerebellar vermis, nucleus accumbens, hippocampus, and amygdala (Figure 3). Our mapping of subcortical dynamics thus provides a gross but more comprehensive depiction of the architecture of human sleep systems, while further supporting electrophysiological and basic research data.

We found that the evolution of the fMRI signal during transition in the hypothalamus and midbrain tegmentum did not coincide. The hypothalamic dynamics was characterized by a lack of the initial signal fall observed in the rest of the brain and by showing the most delayed evolution of the subsequent rise-and-fall signal oscillation. This is evident in Figure 4 and the Supplementary Material Video. Such particular hypothalamic dynamics across the full transition period is consistent with a differentiated role in the regulation of the wake–sleep cycle, as the lateral hypothalamus contains the neurons of the sleep-promoting pathway shutting down the ascending arousal system [1, 4].

The important body of work examining the effects of sedative agents on fMRI measures collectively supports the notion that the brain is functionally reorganized during induced unconsciousness (e.g. [9–21]). Previous studies have regularly involved the comparison of data acquired in wakefulness and unconsciousness rather than the dynamic assessment of the transition point, and thus they are not directly comparable to our data. Nevertheless, a number of observations during natural light sleep are highly consistent with our results. In the initial sleep phase and before slow-wave sleep is fully established, a transient increase in cortico-cortical connectivity has been reported [23, 24], together with significant connectivity reduction between the cortex and the thalamus [23, 26] or the hypothalamus [24]. Importantly, a transient dissociated synchronization may therefore be present in both propofol-induced unconsciousness and natural sleep, which supports a level of generalizability of the results obtained in our study with an unprecedented comprehensive dynamic characterization of the transition phenomenon.

Limitations

Although we initially included 30 participants, the number of valid exams was smaller as a result of motion artifacts. Sample size is a limitation common to fMRI studies examining healthy participants during drug-induced unconsciousness, which is highly complex for both technical and safety reasons. The study was also limited in terms of the assessment of the hypnosis level induced. For obvious reasons, the depth of anesthesia cannot be continuously tested during the MRI acquisition. We used the cessation of a self-paced hand motor task (squeezing an object) as the marker for onset of unconsciousness. This method does not necessarily yield onset times that coincide with the conventional method of assessing the level of consciousness in the context of anesthesia, namely response to verbal command [66]. Likewise, the transition from unconsciousness to wakefulness was not assessed. It would be relevant for future studies to determine whether awaking is also associated with a transient cortico-subcortical dissociation, which would reinforce the notion that large-scale neural dissociation may indicate transition between functionally distinct brain states. Eye status was not monitored during fMRI acquisition. One part of the brain activity changes occurring during the transition period may therefore be related to presumed eye closure. Similarly, some activity changes may relate to ceased hand-pressing movements. Stricto sensu, both events may have introduced bias. However, eye closure and loss of volitional movement may be considered genuine behavioral elements of losing consciousness.

In conclusion, unconsciousness induction with propofol was characterized by a dissociated synchronization at the largest scale of the brain. The cerebral cortex was functionally decoupled from subcortical structures regulating basic aspects of brain activity including the level of consciousness. Such a cortico-subcortical decoupling and subsequent re-coupling may allow the brain to detach from wakeful activity and reorganize into the new state. Elements of the default mode network exceptionally remained connected to the subcortical brain, which would suggest a role of this network in generating a level of consciousness also in the sleep state.

Supplementary Material

Supplementary material is available at *SLEEP* online.

Acknowledgments

The Agency of University and Research Funding Management of Catalonia Government participated in the context of Research Group SGR2017_134 and SGR2017_1198.

Funding

This work was supported in part by the Carlos III Health Institute, Spain (grant number PI16/00616).

Disclosure statement

Financial disclosure: none.
Non-financial Disclosure: none.

References

1. Saper CB, *et al*. Sleep state switching. *Neuron*. 2010;**68**(6):1023–1042.
2. Lee SH, *et al*. Neuromodulation of brain states. *Neuron*. 2012;**76**(1):209–222.
3. Eban-Rothschild A, *et al*. Neuronal mechanisms for sleep/wake regulation and modulatory drive. *Neuropsychopharmacology*. 2018;**43**(5):937–952.
4. Steenland HW. Staying awake: top-down systems control of sleep. *Neurosciences*. 2014;**2**(1):1.
5. Brown EN, *et al*. General anesthesia, sleep, and coma. *N Engl J Med*. 2010;**363**(27):2638–2650.
6. Davis MH, *et al*. Dissociating speech perception and comprehension at reduced levels of awareness. *Proc Natl Acad Sci U S A*. 2007;**104**(41):16032–16037.
7. Murphy M, *et al*. Propofol anesthesia and sleep: a high-density EEG study. *Sleep*. 2011;**34**(3):283–91A.
8. Blumen M, *et al*. Drug-induced sleep endoscopy: a new gold standard for evaluating OSAS? Part I: Technique. *Eur Ann Otorhinolaryngol Head Neck Dis*. 2017;**134**(2):101–107.
9. Boveroux P, *et al*. Breakdown of within- and between-network resting state functional magnetic resonance imaging connectivity during propofol-induced loss of consciousness. *Anesthesiology*. 2010;**113**(5):1038–1053.
10. Huang Z, *et al*. Timescales of intrinsic BOLD signal dynamics and functional connectivity in pharmacologic and neuropathologic states of unconsciousness. *J Neurosci*. 2018;**38**(9):2304–2317.
11. Hudetz AG. General anesthesia and human brain connectivity. *Brain Connect*. 2012;**2**(6):291–302.
12. Liu X, *et al*. Propofol attenuates low-frequency fluctuations of resting-state fMRI BOLD signal in the anterior frontal cortex upon loss of consciousness. *Neuroimage*. 2017;**147**:295–301.
13. Luppi AI, *et al*. Consciousness-specific dynamic interactions of brain integration and functional diversity. *Nat Commun*. 2019;**10**(1):4616.
14. Mhuircheartaigh RN, *et al*. Cortical and subcortical connectivity changes during decreasing levels of consciousness in humans: a functional magnetic resonance imaging study using propofol. *J Neurosci*. 2010;**30**(27):9095–9102.
15. Schröter MS, *et al*. Spatiotemporal reconfiguration of large-scale brain functional networks during propofol-induced loss of consciousness. *J Neurosci*. 2012;**32**(37):12832–12840.
16. Guldenmund P, *et al*. Thalamus, brainstem and salience network connectivity changes during propofol-induced sedation and unconsciousness. *Brain Connect*. 2013;**3**(3):273–285.
17. Monti MM, *et al*. Dynamic change of global and local information processing in propofol-induced loss and recovery of consciousness. *PLoS Comput Biol*. 2013;**9**(10):e1003271.
18. Golkowski D, *et al*. Changes in whole brain dynamics and connectivity patterns during sevoflurane- and propofol-induced unconsciousness identified by functional magnetic resonance imaging. *Anesthesiology*. 2019;**130**(6):898–911.
19. Stamatakis EA, *et al*. Changes in resting neural connectivity during propofol sedation. *PLoS One*. 2010;**5**(12):e14224.
20. Jordan D, *et al*. Simultaneous electroencephalographic and functional magnetic resonance imaging indicate impaired cortical top-down processing in association with anesthetic-induced unconsciousness. *Anesthesiology*. 2013;**119**(5):1031–1042.
21. Zhang J, *et al*. Breakdown in the temporal and spatial organization of spontaneous brain activity during general anesthesia. *Hum Brain Mapp*. 2018;**39**(5):2035–2046.
22. Horovitz SG, *et al*. Low frequency BOLD fluctuations during resting wakefulness and light sleep: a simultaneous EEG-fMRI study. *Hum Brain Mapp*. 2008;**29**(6):671–682.
23. Spoormaker VI, *et al*. Development of a large-scale functional brain network during human non-rapid eye movement sleep. *J Neurosci*. 2010;**30**(34):11379–11387.
24. Tagliazucchi E, *et al*. Decoding wakefulness levels from typical fMRI resting-state data reveals reliable drifts between wakefulness and sleep. *Neuron*. 2014;**82**(3):695–708.
25. Larson-Prior LJ, *et al*. Cortical network functional connectivity in the descent to sleep. *Proc Natl Acad Sci U S A*. 2009;**106**(11):4489–4494.
26. Stevner ABA, *et al*. Discovery of key whole-brain transitions and dynamics during human wakefulness and non-REM sleep. *Nat Commun*. 2019;**10**(1):1035.
27. Nir T, *et al*. Transient subcortical functional connectivity upon emergence from propofol sedation in human male volunteers: evidence for active emergence. *Br J Anaesth*. 2019;**123**(3):298–308.
28. Wen H, *et al*. Broadband electrophysiological dynamics contribute to global resting-state fMRI signal. *J Neurosci*. 2016;**36**(22):6030–6040.
29. Schölvinck ML, *et al*. Neural basis of global resting-state fMRI activity. *Proc Natl Acad Sci U S A*. 2010;**107**(22):10238–10243.
30. Zhao L, *et al*. Global fluctuations of cerebral blood flow indicate a global brain network independent of systemic factors. *J Cereb Blood Flow Metab*. 2019;**39**(2):302–312.
31. Gotts SJ, *et al*. Brain networks, dimensionality, and global signal averaging in resting-state fMRI: hierarchical network structure results in low-dimensional spatiotemporal dynamics. *Neuroimage*. 2020;**205**:116289.
32. Turchi J, *et al*. The basal forebrain regulates global resting-state fMRI fluctuations. *Neuron*. 2018;**97**(4):940–952.e4.
33. Celada P, *et al*. Serotonin modulation of cortical neurons and networks. *Front Integr Neurosci*. 2013;**7**:25.
34. Schwartz MD, *et al*. The neurobiology of sleep and wakefulness. *Psychiatr Clin North Am*. 2015;**38**(4):615–644.
35. Steriade M, *et al*. Thalamocortical oscillations in the sleeping and aroused brain. *Science*. 1993;**262**(5134):679–685.
36. Puig MV, *et al*. Serotonin modulation of prefronto-hippocampal rhythms in health and disease. *ACS Chem Neurosci*. 2015;**6**(7):1017–1025.

37. Mayhew D, *et al*. A review of ASA physical status—historical perspectives and modern developments. *Anaesthesia*. 2019; **74**:373–379.
38. Schnider TW, *et al*. The influence of age on propofol pharmacodynamics. *Anesthesiology*. 1999;**90**(6):1502–1516.
39. Song XW, *et al*. REST: a toolkit for resting-state functional magnetic resonance imaging data processing. *PLoS One*. 2011;**6**(9):e25031.
40. López-Solà M, *et al*. Altered functional magnetic resonance imaging responses to nonpainful sensory stimulation in fibromyalgia patients. *Arthritis Rheumatol*. 2014;**66**(11):3200–3209.
41. Harrison BJ, *et al*. Consistency and functional specialization in the default mode brain network. *Proc Natl Acad Sci U S A*. 2008;**105**(28):9781–9786.
42. Pujol J, *et al*. Traffic pollution exposure is associated with altered brain connectivity in school children. *Neuroimage*. 2016;**129**:175–184.
43. Power JD, *et al*. Methods to detect, characterize, and remove motion artifact in resting state fMRI. *Neuroimage*. 2014;**84**:320–341.
44. Pujol J, *et al*. Does motion-related brain functional connectivity reflect both artifacts and genuine neural activity? *Neuroimage*. 2014;**101**:87–95.
45. Smith SW. *The Scientist and Engineer's Guide to Digital Signal Processing*. 2nd ed. San Diego, CA: California Technical Publishing; 1999: 13–17.
46. Fell J, *et al*. The role of phase synchronization in memory processes. *Nat Rev Neurosci*. 2011;**12**(2):105–118.
47. Buzsáki G, *et al*. Brain rhythms and neural syntax: implications for efficient coding of cognitive content and neuropsychiatric disease. *Dialogues Clin Neurosci*. 2012;**14**(4):345–367.
48. Kiviniemi VJ, *et al*. Midazolam sedation increases fluctuation and synchrony of the resting brain BOLD signal. *Magn Reson Imaging*. 2005;**23**(4):531–537.
49. Licata SC, *et al*. The hypnotic zolpidem increases the synchrony of BOLD signal fluctuations in widespread brain networks during a resting paradigm. *Neuroimage*. 2013;**70**:211–222.
50. Zuo XN, *et al*. The oscillating brain: complex and reliable. *Neuroimage*. 2010;**49**(2):1432–1445.
51. Wright KP Jr, *et al*. Topographical and temporal patterns of brain activity during the transition from wakefulness to sleep. *Sleep*. 1995;**18**(10):880–889.
52. Sanders RD, *et al*. Unresponsiveness ≠ unconsciousness. *Anesthesiology*. 2012;**116**(4):946–959.
53. Tononi G, *et al*. The neurology of consciousness: an overview. In: Laureys S, Gosseries O, Tononi G (eds.). *The Neurology of Consciousness: Cognitive Neuroscience and Neuropathology*. 2nd ed. San Diego, CA: Elsevier Ltd; 2016:16–22.
54. Moll J, *et al*. The self as a moral agent: linking the neural bases of social agency and moral sensitivity. *Soc Neurosci*. 2007;**2**(3–4):336–352.
55. Bado P, *et al*. Functional dissociation of ventral frontal and dorsomedial default mode network components during resting state and emotional autobiographical recall. *Hum Brain Mapp*. 2014;**35**(7):3302–3313.
56. Leech R, *et al*. The role of the posterior cingulate cortex in cognition and disease. *Brain*. 2014;**137**(Pt 1):12–32.
57. Pujol J, *et al*. The contribution of brain imaging to the understanding of psychopathy. *Psychol Med*. 2019;**49**(1):20–31.
58. Liu X, *et al*. Variation of the default mode network with altered alertness levels induced by propofol. *Neuropsychiatr Dis Treat*. 2015;**11**:2573–2581.
59. Bharath RD, *et al*. Dynamic local connectivity uncovers altered brain synchrony during propofol sedation. *Sci Rep*. 2017;**7**(1):8501.
60. Liu X, *et al*. Increased precuneus connectivity during propofol sedation. *Neurosci Lett*. 2014;**561**:18–23.
61. Amico E, *et al*. Posterior cingulate cortex-related co-activation patterns: a resting state FMRI study in propofol-induced loss of consciousness. *PLoS One*. 2014;**9**(6):e100012.
62. Horovitz SG, *et al*. Decoupling of the brain's default mode network during deep sleep. *Proc Natl Acad Sci U S A*. 2009;**106**(27):11376–11381.
63. Dresler M, *et al*. Volitional components of consciousness vary across wakefulness, dreaming and lucid dreaming. *Front Psychol*. 2014;**4**:987.
64. Siclari F, *et al*. Dreaming in NREM sleep: a high-density EEG study of slow waves and spindles. *J Neurosci*. 2018;**38**(43):9175–9185.
65. Radek L, *et al*. Dreaming and awareness during dexmedetomidine- and propofol-induced unresponsiveness. *Br J Anaesth*. 2018;**121**(1):260–269.
66. Chernik DA, *et al*. Validity and reliability of the Observer's Assessment of Alertness/Sedation Scale: study with intravenous midazolam. *J Clin Psychopharmacol*. 1990;**10**(4):244–251.